The 2010 IEEE/RSJ International Conference on
Intelligent Robots and Systems
October 18-22, 2010, Taipei, Taiwan

Motion Planning for Dynamic Knotting of a Flexible Rope with a High-speed Robot Arm

Yuji Yamakawa, Akio Namiki and Masatoshi Ishikawa

***Abstract*— In this paper, we propose an entirely new strategy for dexterous manipulation of a linear flexible object with a high-speed robot arm. The strategy involves manipulating the object at high speed. By moving the robot at high speed, we can assume that the dynamic behavior of the linear flexible object can be obtained by performing algebraic calculations of the robot motion. Based on this assumption, we derive a model of the linear flexible object and confirm the validity of the proposed model. Finally, we perform simulation of dynamic knotting based on the proposed model. Results of an experiment demonstrating dynamic knotting with a high-speed robot arm are shown.**

I. Introduction

Object manipulation is an extremely important problem in the robotics field. Until now, many researchers have proposed manipulation techniques to achieve various tasks.

A. Manipulation skill

Robotic manipulation can be divided into four types (see Fig. 1): "Static manipulation of a rigid object", "Static manipulation of a flexible object", "Dynamic manipulation of a rigid object", and "Dynamic manipulation of a flexible object"

Static manipulation of a rigid object This manipulation can be performed with a stable grasping state, and various tasks have been achieved. For instance, Harada et al. demonstrated rolling-based manipulation of multiple objects [1].

Static manipulation of a flexible object The knotting of a linear flexible object has been demonstrated by some researchers. For example, Inaba et al. proposed a method of knotting a rope with a manipulator [2]. Matsuno et al. used an imaging system to recognize the shape of a rope and demonstrated knotting using dual manipulators [3]. In addition, we have proposed a knotting strategy and visual and tactile sensory feedback control for high-speed knotting [4].

Dynamic manipulation of a rigid object As one example of dynamic manipulation, Lynch and Mason demonstrated posture translation of a rigid object using rotary motion of the object [5]. In our laboratory, batting, dribbling, dynamic regrasping, and pen spinning have been achieved by using a high-speed robot and high-speed visual and tactile sensory feedback [6].

Y. Yamakawa and M. Ishikawa are with the Dept. of Information Physics and Computing, Graduate School of Information Science and Technology, Univ. of Tokyo, 7-3-1 Hongo, Bunkyo-ku, Tokyo 113-8656, Japan. Yuji_Yamakawa@ipc.i.u-tokyo.ac.jp

A. Namiki is with the Dept. of Mechanical Engineering, Division of Artificial Systems Science, Graduate School of Engineering, Chiba University, 1-33 Yayoi-cho, Inage-ku, Chiba 263-8522, Japan. namiki@faculty.chiba-u.jp

Manipulation / Object	Static Manipulation	Dynamic Manipulation
Rigid Body	stable grasping	high-speed visual and tactile feedback
Flexible Body	trajectory generation with visual feedback	???

Fig. 1. Comparison of types of manipulation.

Dynamic manipulation of a flexible object Hashimoto et al. deformed the rope to the desired configuration using a rope dynamic model [7]. Suzuki et al. performed grasping manipulation by twisting a rope around an object [8]. Mochiyama et al. described the kinematics and dynamics of a hyper-flexible manipulator [9]. In these studies, trajectory planning and a control method based on a dynamic model of the flexible object were proposed. However, since the proposed model is quite complex, the control method based on the model is also complex and is not robust against modeling errors. Moreover, practical examples of dynamic manipulation of a flexible object, such as knotting of a rope, have not been achieved in these studies. We consider that these manipulations are far from the dexterous manipulation of a flexible rope.

As described above (Fig. 1), static manipulation of rigid and flexible objects and dynamic manipulation of a rigid object have already been achieved. However, the dynamic manipulation of a flexible object has not been executed actively. Thus, we consider that an effective strategy and control method for the dynamic manipulation of a flexible object should be proposed in order to improve the manipulation ability.

B. Dynamic manipulation of a flexible object

The difficulties faced in dynamic manipulation of a flexible object include:

- Deformation of the object during manipulation.
- The difficulty of estimating the object's deformation.

We expect that research on this kind of manipulation will be stimulated by proposing a method that solves these difficulties. As one solution, high-speed motion and high-speed sensory feedback are considered. With this approach, motion planning of the high-speed robot in particular is extremely important.

Many motion planning methods for flexible manipulators have been suggested. For instance, Arisumi et al. proposed

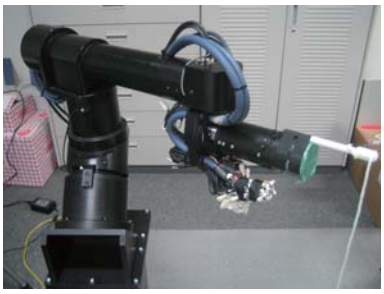

(a) Photograph of high-speed robot arm

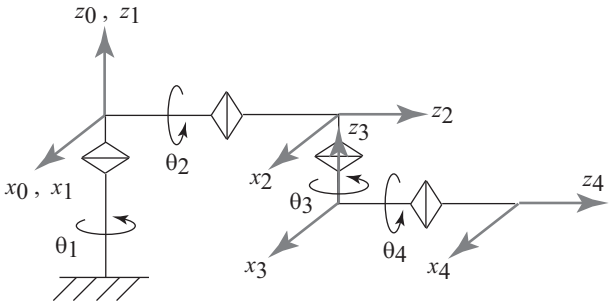

(b) reference configuration

Fig. 2. High-speed robot arm.

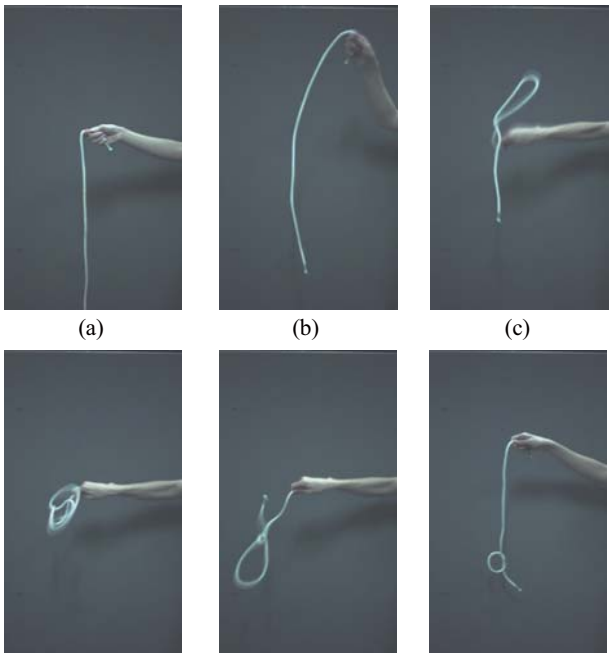

Fig. 3. Dynamic knotting by a human subject.

casting manipulation [10], Yahya et al. performed motion planning based on a geometrical method [11], and Mohri et al. executed efficient motion planning using a performance index [12]. However, motion planning for manipulation of a flexible object has not been discussed.

Therefore, here we propose a novel strategy using the high-speed motion of a robot arm to solve the above problems. By using the high-speed motion, we assume that the rope deformation can be derived algebraically from the robot motion. The goal of this study is to show that the model and the control method of a linear flexible object can be simplified by using the high-speed performance of the robot and sensors. As a concrete manipulation task, dynamic knotting of a flexible rope is demonstrated.

II. System Configuration

Fig. 2(a) shows a photograph of the high-speed robot arm. The robot arm has five degrees of freedom, including the oblique axis, the rotation axis (θ_1) of the upper arm (shoulder), the circulation axis (θ_2) of the upper arm, the rotation axis (θ_3) of the lower arm (elbow), and the circulation axis (θ_4) of the lower arm. The actuators are high-power devices for realizing high-speed movement; for example, the maximum velocity of the elbow is 15.83 m/s, and the maximum velocity of the end-effector is 27.22 m/s. Since the velocity of the human arm (elbow) is about 6–10 m/s, the motion of the manipulator is as fast and flexible as human motion. Fig. 2(b) shows the kinematics and the base coordinates in the robot arm, with the exception of the oblique axis. The joint angles are controlled to the desired angles by PD control. The sampling rate of the control system is 1 kHz.

A stick is attached to the robot arm, and a flexible rope is attached to the stick, as shown in Fig. 2(a).

III. Analysis of Dynamic Knotting

In this section, we explain the analysis of dynamic knotting of a flexible rope. First, dynamic knotting by a human subject is analyzed in order to extract the arm motion that achieves the dynamic knotting. Fig. 3 shows a sequence of continuous photographs of dynamic knotting performed by the human subject. Fig. 3(a) shows the initial state, Fig. 3(b) shows moving of the rope using shoulder motion, Fig. 3(c) shows loop production using shoulder and elbow motions, Fig. 3(d) $\sim$ (e) show the rope moving through the loop using the rope inertia when the rope sections collide, and Fig. 3(f) shows the final state where dynamic knotting is completed. As a result, dynamic knotting using deformation of the rope will be achieved by a combination of shoulder motion and elbow motion. Fig. 4 shows an overall image of the dynamic knotting and the high-speed arm motion. Since the success rate for human subjects learning how to perform this knotting is about 15 %, this task requires extremely difficult and dexterous manipulation.

In this task, loop production on the rope and collision of the rope sections at an intersection of the loop are extremely important elements. Thus, it is important to perform motion planning of the robot arm so as to carry out these tasks. In this study, the tip trajectory obtained from the human knotting is not used. We propose a method in which motion planning of the arm can be obtained from a given rope configuration. This motion planning method can be applied to various tasks involving dynamic manipulation of flexible objects.

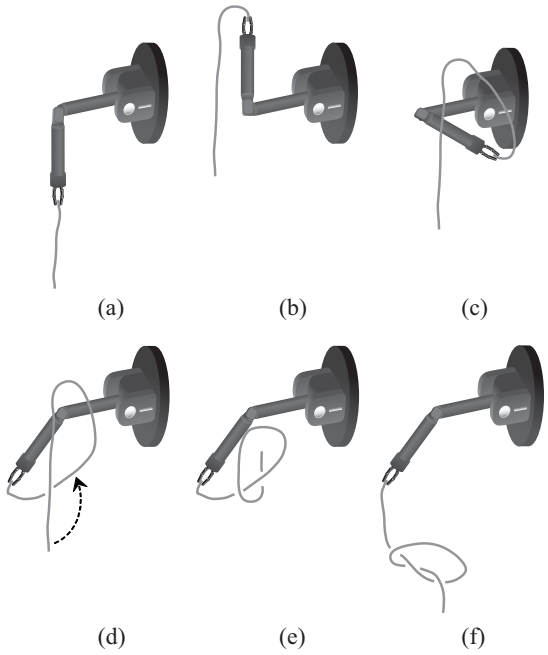

Fig. 4. Strategy of dynamic knotting.

IV. Modeling and Simulation

In this section, a rope model will be derived in order to generate a robot trajectory, verify the validity of the robot trajectory, calculate the deformation of the rope, and propose a control scheme.

As can be seen from the dynamic knotting performed by the human subject, shown in Fig. 3 (a)–(c), the rope section located at the "far" position from the part grasped by the human does not move during the high-speed motion. On the other hand, the rope section located at the "near" position from the grasped part deforms so as to track the human arm motion.

From the above discussion, the rope deformation depends on the high-speed robot motion. As a result, we can assume that the rope deformation can be derived algebraically from the robot motion. Thus, the rope deformation model can be described as a relational expression (static model) derived from the robot motion in this study. Also, since the rope deformation can be calculated algebraically from the robot motion, the model of the rope deformation will be more simple than typical models [7], [8], [9].

If the dynamic manipulation is performed in slow motion, gravity effectively acts on the rope. In that case, the algebraic equation does not hold, and we have to consider a differential equation. As a result, dynamic manipulation in slow motion is extremely difficult. Thus, high-speed robot motion is required in order to achieve dynamic manipulation.

A. Kinematics of robot arm

Here we consider the kinematics (Fig. 2) in order to derive the tip position of the robot arm. Since the tip position of the robot arm does not depend on the joint angle of the circulation axis (θ_4) of the lower arm, this joint angle can be neglected. The joint angles and the tip position of the robot arm are defined by $\boldsymbol{\theta} \in \boldsymbol{R}^3$ and $\boldsymbol{r} \in \boldsymbol{R}^3$, respectively. In general, the relationship between the tip position and the joint angles can be obtained by the following equation.

$$\boldsymbol{r}(t) = \boldsymbol{f}(\boldsymbol{\theta}(t)). \tag{1}$$

Although the details of the derivation are omitted, the tip position is derived by using the Denabit-Hartenburg description.

B. Deformation model of rope

A rope model is frequently described by a distributed parameter system (partial differential equation). In other models, the rope is approximated by a multi-link system, and the equation of motion (ordinary differential equation) for each joint is derived. In this research, we apply the multi-link system to the rope model. Then, the equation of motion can be replaced by an algebraic equation under the constraint of high-speed motion of the robot.

The following facts can be assumed in the rope deformation model.

1) The behavior of the rope section located at the "near" position from the part grasped by the robot arm does depend on the robot motion.
2) The behavior of the rope section located at the "far" position from the part grasped by the robot arm does not depend on the robot motion.
3) The distance between two joint coordinates of the rope is not variable.
4) There is a time delay between robot motion and the subsequent rope deformation.
5) Twisting of the rope is not taken into account.

The first assumption means that the rope deformation can be given by the tip position of the robot arm, and the second assumption means that rope deformation does not occur even if the robot arm moves. The third assumption is the constraint that the link distance in the multi-link model does not change. The fourth assumption means that even if the robot moves, the rope section located at the far position from the grasped position does not deform during the time delay.

From the above conditions, we assume that the rope deformation can be algebraically represented by the following equation:

$$\boldsymbol{s}_i(t) = \boldsymbol{r}(t - d_i), \tag{2}$$

where i is the joint number of the rope ($i = 1, 2, \cdots, N = 20$); $\boldsymbol{s}_i \in \boldsymbol{R}^3$ ("3" means $[x\ y\ z]$ coordinates) is the i-th joint coordinate of the rope; and d_i is the time delay ($d_i = \lambda l(i-1)$ on the i-th joint, where λ (=1.2) is a normalized time delay and l is the link distance). The first joint is set at the position grasped by the robot. As a result, the time delay d_1 is equal to zero.

Since the proposed model does not include an inertia term, Coriolis and centrifugal force terms, or a spring term, we do not need to estimate the dynamic model parameters; only the normalized time delay λ has to be estimated. The value of λ may be dependent on the characteristics of the rope. The advantage of the proposed model is that the number of

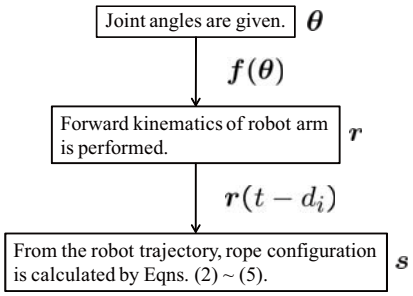

Fig. 5. Simulation flow of forward problem.

model parameters is lower than one of the typical models. Therefore, the proposed model itself is robust. Moreover, since the rope model can be algebraically calculated, the simulation time becomes much shorter.

C. Correction of distance between two joint coordinates

Describing the rope deformation using Eqn. (2), there exists a case where the distance between two joint coordinates cannot be kept constant. Therefore, in order to satisfy assumption 3), the joint coordinates of the rope need to be converted as follows:

The joint coordinate to be converted is defined as $\boldsymbol{s}_i = [x_i \quad y_i \quad z_i]$, and the prior (that is, nearer to the position grasped by the robot) joint coordinate is $\boldsymbol{s}_{i-1} = [x_{i-1} \quad y_{i-1} \quad z_{i-1}]$. The distance between these two joint coordinates can be described by

$$D = \| \boldsymbol{s}_i - \boldsymbol{s}_{i-1} \| . \tag{3}$$

In the case where D is not equal to l (l is the link distance), the joint coordinate $\boldsymbol{s}_i$ is corrected in terms of polar coordinates as follows:

$$\begin{aligned} x_i &= l \sin\theta \cos\phi + x_{i-1} \\ y_i &= l \sin\theta \sin\phi + y_{i-1} \\ z_i &= l \cos\theta + z_{i-1} \end{aligned} \tag{4}$$

where

$$\begin{aligned} \theta &= \cos^{-1}\left(\frac{z_i - z_{i-1}}{D}\right) \\ \phi &= \cos^{-1}\left(\frac{x_i - x_{i-1}}{\sqrt{(x_i - x_{i-1})^2 + (y_i - y_{i-1})^2}}\right). \end{aligned} \tag{5}$$

Fig. 5 shows the simulation flow of the forward problem. First, the joint angles of the robot arm are given. Then, the tip position of the robot arm is calculated by the forward kinematics. Finally, the rope deformation is derived by Eqns. (2)–(5).

D. Validation of model

Here, a simple simulation (rope vibration) will be executed in order to confirm the validity of the proposed model. In this simulation, the length of the rope is 0.5 m. Since the number of joints N of the multi-link rope model is 20, the link distance l is 0.025 m. The amplitude and frequency of the sinusoidal motion are 2 deg and 5 Hz. Fig. 6 and Fig. 7 show the experimental result and simulation result for the sinusoidal motion of the arm, respectively. As can be seen from these figures, the dynamic behaviors of both results are about the same. Thus, the validity of the proposed model of the rope deformation can be confirmed.

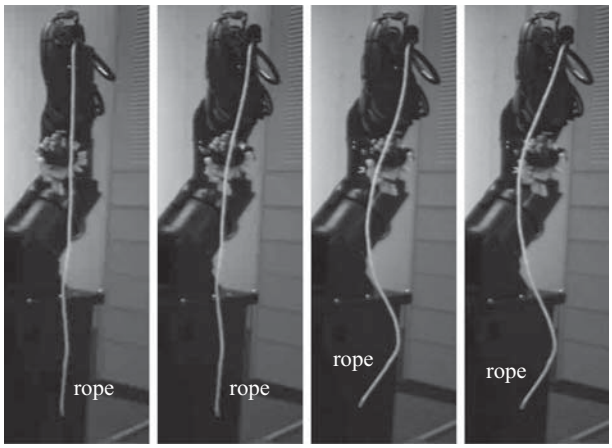

(a) t = 0 sec (b) t = 0.05 sec (c) t = 0.25 sec (d) t = 0.45 sec

Fig. 6. Experimental result of sinusoidal motion.

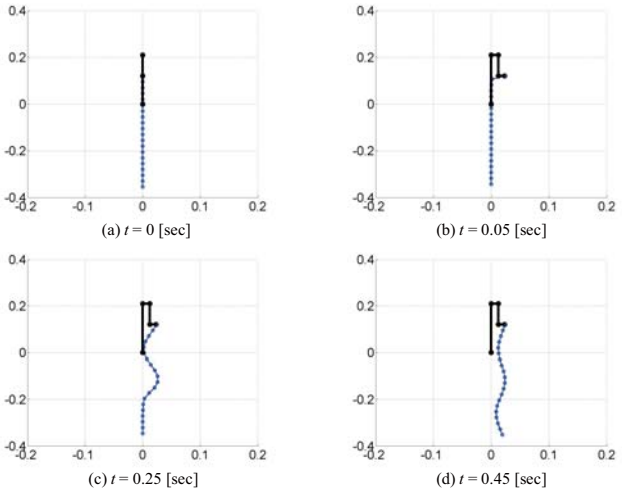

Fig. 7. Simulation result of sinusoidal motion.

E. Inverse problem

This section explains the inverse problem of deriving the joint angles of the robot arm from the rope configuration. Fig. 8 shows the simulation flow of the inverse problem.

First, we give the number of links of the multi-link system of the rope. The desired rope configuration ($\boldsymbol{s}$) is graphically given in a two-dimensional plane by a human. Here, there exists a case where the link distance between the two joint coordinates on the given rope configuration is not equal to l. Therefore, the rope configuration is corrected using the polar coordinates (Eqns. (3) $\sim$ (5)).

Second, the rope configuration ($\boldsymbol{s_r}$) is converted so as to match the robot arm kinematics to avoid problems such as a singular point.

Third, the trajectory of the tip position ($\boldsymbol{r}$) of the robot

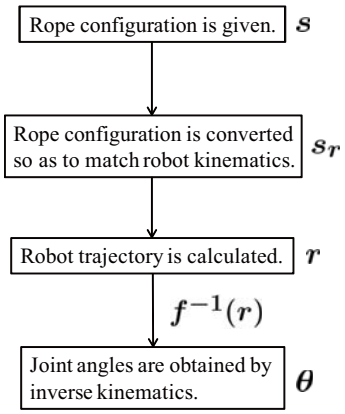

Fig. 8. Simulation flow of inverse problem.

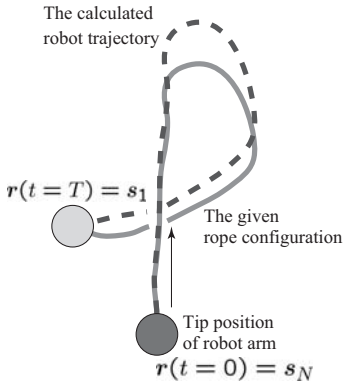

Fig. 9. Compensation for the effects of gravity.

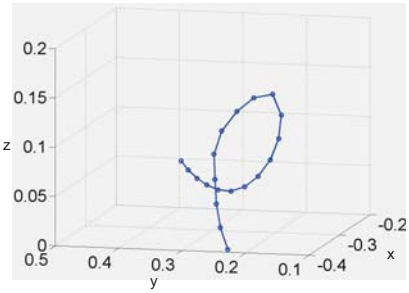

Fig. 10. Rope configuration.

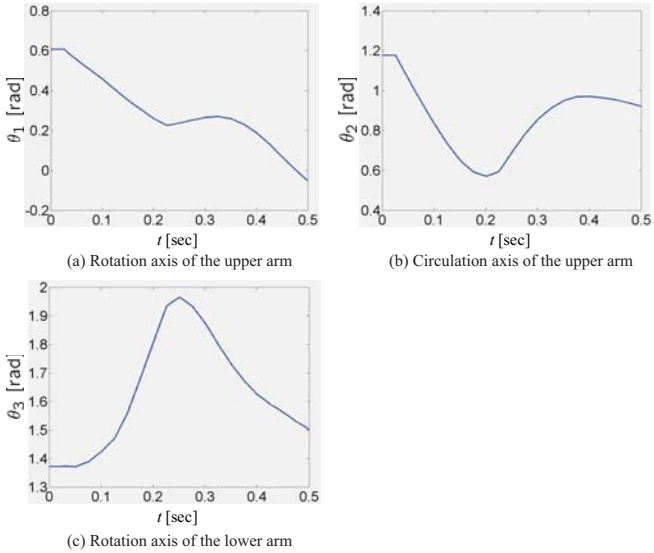

(a) Rotation axis of the upper arm
(b) Circulation axis of the upper arm
(c) Rotation axis of the lower arm

Fig. 11. Joint trajectory of robot arm.

arm is calculated from the converted rope configuration (s_r). From the assumption that the rope deformation depends on the high-speed arm motion, the trajectory (r) of the robot arm can be obtained, to track the given coordinate of each joint of the rope. Namely, we have the following equations:

$$r(t=0)=s_N, \quad r(t=T)=s_1, \tag{6}$$

where N (=20) is the number of joints, and T (=0.5 s) is the motion time. The trajectory is determined so as to linearly move from the N-th link to the first link during the motion time T. Here, the trajectory is calculated so as to compensate for the effects of gravity (Fig. 9).

Finally, the joint angles (θ) of the robot arm can be obtained by solving the inverse kinematics.

F. Simulation of dynamic knotting

In this section, the simulation results of dynamic knotting by the robot arm are shown. The simulation conditions are the same as those used in the above section.

In order to achieve dynamic knotting of the rope, motion planning of the robot arm is extremely important. In particular, loop production on the rope and contact of the rope sections at the intersection of the loop are key elements to the success of this task. Thus, motion planning is required so as to perform these elements.

In this simulation, the rope configuration (s_r) is given as shown in Fig. 10. Then, the joint angles (θ) of the robot arm can be calculated by solving the inverse kinematics. Fig. 11 shows the results of the joint trajectory of the robot arm. From these results, smooth trajectories of the joint angles can be obtained. Fig. 12 shows the simulation results of the forward problem using the joint angles obtained by the inverse problem. From this result, the same configuration as the given rope configuration is obtained. Namely, the joint trajectory obtained by the simulation can be used in the experiment. In addition, it can be confirmed that loop production on the rope and contact of rope sections in the loop are achieved. By using the proposed model, the trajectory of the robot arm can be algebraically obtained when an arbitrary rope configuration is given.

In the next section, we will show the experimental results of dynamic knotting of a flexible rope by the high-speed robot arm.

V. Experiment

Fig. 13 shows the experimental results of dynamic knotting by the high-speed robot arm. In this experiment, the joint trajectories of the robot arm obtained from the simulation result are used, and the diameter and the length of the rope are 3 mm and 0.5 m, respectively. It can be seen from Fig. 13 that dynamic knotting of the flexible rope can be achieved. Since the execution time is 0.5 s, knotting can be carried out

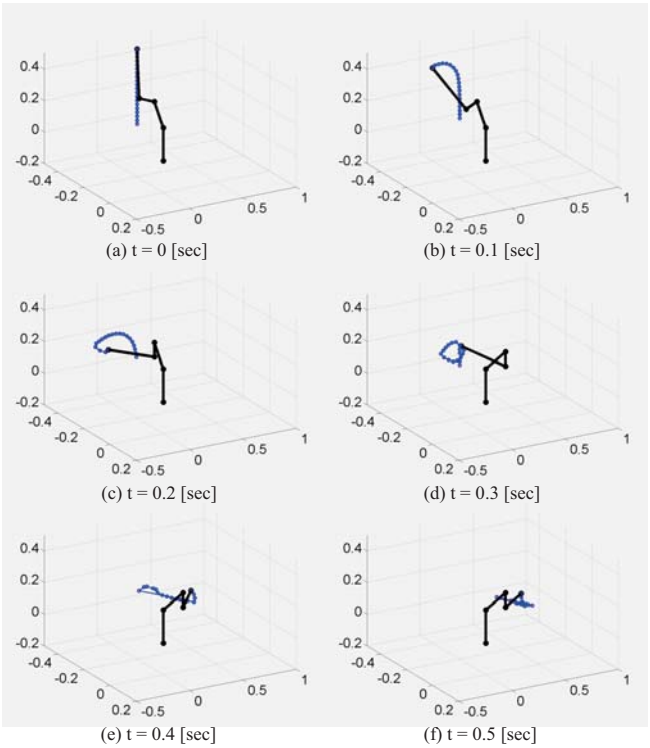

Fig. 12. Simulation result of dynamic knotting.

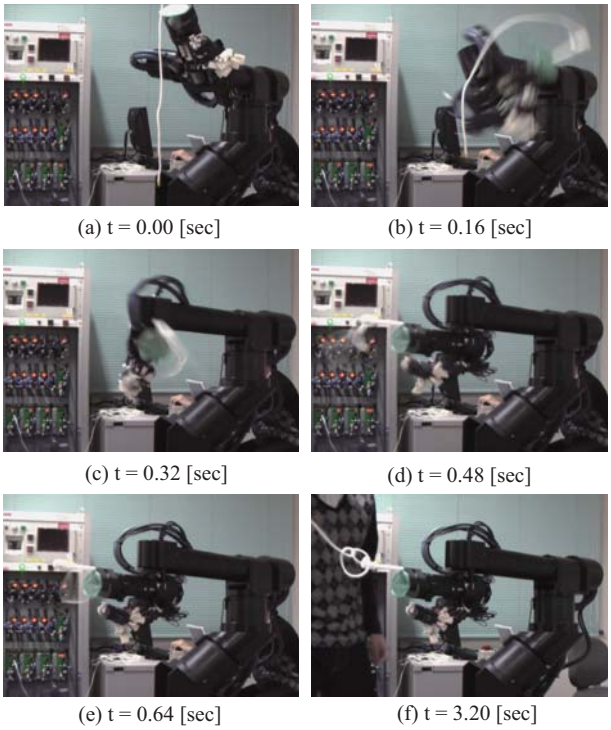

Fig. 13. Continuous sequence of photographs of dynamic knotting.

at high speed. This video sequence can be viewed on our web site [13]. In the last 1 s of this video, the human subject completes the knotting. However, this part was merely to make it easier to see the knot and is not essential in this study.

The success rate of the experiment was about 20 %. This success rate is higher than that of human dynamic knotting. Therefore, the validity of the proposed model and the joint trajectory obtained by the simulation can be confirmed. Moreover, it can be considered that motion planning of the robot arm is extremely beneficial. Possible causes of failure include twisting of the rope, the initial conditions, and the contact timing of the rope sections. The success rate will be improved by introducing high-speed visual feedback.

VI. Conclusions

The aim of this research is the dynamic manipulation of a flexible object. As one example, the dynamic knotting of a flexible rope by a high-speed robot arm is considered. In the dynamic manipulation of the flexible object, the deformation of the object during the manipulation complicates the modeling and control of the flexible object.

In this paper, the dynamic model of the flexible rope can be boiled down to the choice of algebraic model based on the high-speed motion of the robot. Based on this consideration, we proposed an algebraic rope model calculated from the robot motion. The validity of the proposed model was confirmed. Motion planning of the robot arm was achieved by using the proposed model when an arbitrary rope configuration was given. Experimental results are shown.

In future work, we plan to introduce a high-speed visual feedback system in order to improve the success rate.

References

[1] K. Harada, M. Kaneko, and T. Tsuji, Rolling-Based Manipulation for Multiple Objects, *Proc. IEEE Int. Conf. on Robotics and Automation*, pp. 3887–3894, 2000.
[2] H. Inoue and M. Inaba, Hand-eye Coordination in Rope Handling, *Robotics Research: The First International Symposium, MIT Press*, pp. 163–174, 1984.
[3] T. Matsuno, T. Fukuda, and F. Arai, Flexible Rope Manipulation by Dual Manipulator System Using Vision Sensor, *Proc. IEEE/ASME Int. Conf. on Advanced Intelligent Mechatronics*, pp. 677–682, 2001.
[4] Y. Yamakawa, A. Namiki, M. Ishikawa, and M. Shimojo, One-Handed Knotting of a Flexible Rope with a High-Speed Multifingered Hand having Tactile Sensors, *Proc. IEEE/RSJ 2007 Int. Conf. on Intelligent Robots and Systems*, pp. 703–708, 2007.
[5] K.M. Lynch and M.T. Mason, Dynamic Nonprehensile Manipulation: Controllability, Planning, and Experiments, *Int. Journal of Robotics Research*, Vol. 18, No. 1, pp. 64–92, 1999.
[6] http://www.k2.t.u-tokyo.ac.jp/fusion/
[7] M. Hashimoto and T. Ishikawa, Dynamic Manipulation of Strings for Housekeeping Robots, *Proc. IEEE Int. Workshop on Robot and Human Interactive Communication*, pp. 368–373, 2002.
[8] T. Suzuki, Y. Ebihara, and K. Shintani, Dynamic Analysis of Casting and Winding with Hyper-Flexible Manipulator, *Proc. IEEE Int. Conf. on Advanced Robotics*, pp. 64–69, 2005.
[9] H. Mochiyama and T. Suzuki, Kinematics and Dynamics of a Cable-like Hyper-flexible Manipulator, *Proc. IEEE Int. Conf. on Robotics and Automation*, pp. 3672–3677, 2002.
[10] H. Arisumi, T. Kotoku and K. Komoriya, A Study of Casting Manipulation (Swing Motion Control and Planning of Throwing Motion). *Proc. IEEE/RSJ 1997 Int. Conf. on Intelligent Robots and Systems*, pp. 168–174, 1997.
[11] S. Yahya, H. A. F. Mohamed and M. Moghavvemi, Motion Planning of Hyper Redundant Manipulators Based on a New Geometrical Method. *Proc. Int. Conf. on Industrial Technology*, 2009.
[12] A. Mohri, P. K. Sarkar and M. Yamamoto, An Efficient Motion Planning of Flexible Manipulator along Specified Path. *Proc. IEEE Int. Conf. on Robotics and Automation*, pp. 1104–1109. 1998.
[13] http://www.k2.t.u-tokyo.ac.jp/fusion/DynamicKnotting/